



OPEN Neurobiological correlates of personality dimensions in borderline personality disorder using graph analysis of functional connectivity

Francesca D'Adda^{1,9}, Giovanni Sighinolfi^{2,9}, Micaela Mitolo^{2,3}, Mauro Scala^{4,5,6}, Lucia Guidi², Lorenzo Motta², Lorenzo Cirignotta⁷, David Neil Manners^{2,8}, Caterina Tonon^{2,4,✉}, Raffaele Lodi^{2,4,9} & Marco Menchetti^{4,9}

Borderline personality disorder (BPD) is a type B personality disorder primarily characterized by a pattern of unstable interpersonal relationships, a distorted self-concept, and intense emotional reactions, associated with extreme and opposing mental and behavioral states, which coexist and lead to destructive behaviors such as self-harm, commonly recurring over time.. The Personality Inventory for the Diagnostic and Statistical Manual of Mental Disorders (DSM), Fifth Edition (PID-5) provides a dimensional assessment of maladaptive domains associated with personality disorders, improving the understanding of their complex clinical presentations. While altered brain functional connectivity (FC) has been reported in BPD, neurobiological-clinical correlations remain debated. This study explores the relationship between the personality dimensions of BPD and resting-state fMRI (rs-fMRI) FC. Twenty-eight patients with BPD (6M/22F, 23.7 ± 3.4 years) and twenty-eight matched healthy controls (6M/22F, 24.3 ± 2.8 years) underwent a psychiatric assessment, including the PID-5, and an MRI protocol including rs-fMRI. Functional data were analyzed via graph theory to derive network properties at global and nodal levels, which were correlated with the PID-5 subdomains. The results revealed impairments across all personality trait facets. Patients had lower global connectivity and compromised centrality of several limbic structures and frontotemporal regions. Significant correlations were found between separation insecurity and global efficiency ($R = 0.60$, adjusted- $p = 0.035$) and between depressivity and the degree of the left middle temporal gyrus ($R = 0.69$, adjusted- $p = 0.023$) in females. These findings suggest links between negative affectivity traits, in particular separation insecurity and depressivity, and specific brain network dysfunctions in BPD.

Keywords Borderline personality disorder, Personality inventory for DSM-5, Graph analysis, Functional magnetic resonance imaging, Functional connectivity

Borderline personality disorder (BPD) is a complex type B personality disorder characterized by affective and interpersonal instability and self-perception disturbance¹. It often presents with dysphoria, emotion dysregulation, anger rumination, impulsivity, self-injury, and suicidal attempts². Subgroups within BPD have been identified, including an "extrovert/externalizing" type characterized by traits linked to histrionic, narcissistic, or antisocial personality disorders, and a smaller subgroup with marked schizotypal and paranoid

¹Department of Mental Health and Pathological Dependencies, Local Health Authority of Bologna, Bologna, Italy.

²IRCCS Istituto delle Scienze Neurologiche di Bologna, Bologna, Italy. ³Department of Medicine and Surgery, University of Parma, Parma, Italy. ⁴Department of Biomedical and Neuromotor Sciences (DIBINEM), University of Bologna, Bologna, Italy. ⁵Psychiatry Department, Health Research Institute Hospital, 12 de Octubre (Imas 12), Madrid, Spain. ⁶Complutense University of Madrid (UCM), Madrid, Spain. ⁷Department of Medicine and Surgery (DIMEC), University of Bologna, Bologna, Italy. ⁸Department for Life Quality Sciences, University of Bologna, Bologna, Italy. ⁹Francesca D'Adda, Giovanni Sighinolfi, Raffaele Lodi and Marco Menchetti contributed equally to this work. ✉email: caterina.tonon@unibo.it

features. The inherent complexity of BPD significantly challenges treatment efforts, with only 50% of patients achieving recovery within a decade of diagnosis³. Moreover, BPD results in persistent impairments in social and occupational functioning, exacerbating the burden of the disorder³.

To address these challenges, the Alternative Model for Personality Disorders (AMPD) was introduced in the fifth edition of the Diagnostic and Statistical Manual of Mental Disorders (DSM-5)⁴. This model provides a flexible and precise framework that shifts the focus from rigid diagnostic criteria to the assessment of personality dysfunction and maladaptive traits, promoting a dimensional approach to diagnosis and research⁵.

This model is particularly relevant for studying complex conditions such as BPD, as it captures individual differences in traits and functioning that previous diagnostic methods may overlook. The AMPD includes tools such as the Personality Inventory for DSM-5 (PID-5), which evaluates maladaptive personality traits described as 25 facets grouped in 5 domains (see Table 1 for a detailed description), similarly featuring the Big Five Personality dimensions⁶. Specifically, patients with BPD commonly present with an impairment in the domains of negative affectivity and disinhibition; emotional lability, impulsivity, depressivity, and hostility are the most predictive facets of BPD⁴. The PID-5 demonstrated significant utility in assessing traits associated with BPD, achieving a sensitivity of 81% and specificity of 76% when applied to BPD diagnostic frameworks, highlighting its effectiveness in identifying the previously mentioned core maladaptive traits⁷. Hence, compared to traditional diagnostic models, such as those defined by the DSM-5, the PID-5's dimensional framework offers a more detailed and systematic approach to evaluating personality pathology⁷.

Despite its high prevalence, the neurobiological underpinnings of BPD remain poorly understood, posing challenges for diagnosis and treatment. While recent neurobiological research identified structural and functional brain changes associated with BPD, evidence linking neurobiological findings to the clinical features of the disorder remains limited and contradictory.

One major area of investigation focuses on abnormalities in fronto-limbic circuits, which are critical for emotion regulation and impulsivity, core symptoms of BPD⁸. Morphometric, functional and structural alterations were detected using multimodal magnetic resonance imaging (MRI)^{9–11}, revealing reductions in gray matter volume (GMV) in regions such as the amygdala¹², anterior cingulate cortex (ACC), orbitofrontal cortex (OFC), dorsolateral and medial prefrontal cortex (dlPFC and mPFC)¹³, and hippocampus¹⁴. A reduction in cortical thickness was also observed in the insular cortex¹⁵, correlating with psychopathological features such as violent and impulsive behavior, in advanced stages of BPD¹⁶. Similarly, decreased GMV in the prefrontal regions, particularly the ACC were associated with emotional dysregulation and impulsivity^{12,17}. However, contrasting results revealed an increase in the GMV in limbic structures¹⁷.

In these studies, clinical assessment was performed using psychometric tools such as the Borderline Symptom List-23 (BSL-23), the Barratt Impulsive Scale-11 (BIS-11), and the Difficulty in Emotion Regulation Scale (DERS). However, these tools lack the comprehensive dimensional approach offered by the PID-5.

Functional alterations have also been studied using resting-state functional magnetic resonance imaging (rs-fMRI), which investigates brain connectivity at rest¹¹. Rs-fMRI data can be analyzed via a variety of approaches; an introduction to these methods is described by Smitha et al.¹⁸. Among them, graph analysis is currently a widely used technique that is based on generating a model of the brain as a set of nodes (brain regions) connected between each other through links describing their “functional connectivity” (FC). The resulting networks are investigated on the basis of a consolidated mathematical theory, the graph theory, which provides an in-depth characterization of the network structure and connectivity^{19,20}. An exemplary application of this technique in BPD patients is presented by Xu et al.²¹, where altered connectivity features are observed at the whole-network level, as well as locally in key limbic (amygdala, entorhinal cortex) and several frontotemporal areas, as supported by other findings^{22–24}. Further studies have reported the pathological involvement of the default mode and salience networks^{24–26}.

While MR studies identified consistent structural changes in brain regions implicated in BPD, the relationship between neurobiological correlates and the clinical features of BPD remains unclear¹⁷. Furthermore, despite the considerable potential of the PID-5, few clinical studies have used this psychometric tool in samples of patients with BPD¹.

In this study, we aim to address these gaps by investigating the correlation between key personality traits, as defined by the PID-5, and alterations in brain connectivity identified through rs-fMRI. By using the dimensional framework of the PID-5, this research aims to provide a more detailed understanding of how personality traits are linked to specific neurobiological patterns in BPD. Ultimately, this approach may advance diagnostic accuracy and guide the development of more effective, personalized treatments for individuals with BPD.

Negative affect	Detachment	Antagonism	Disinhibition	Psychoticism
Emotional Lability; Anxiousness; Separation Insecurity; Hostility; Perseveration; Restricted Affectivity; Submissiveness	Withdrawal; Anhedonia; Intimacy Avoidance; Depressivity; Suspiciousness	Manipulativeness; Deceitfulness; Grandiosity; Attention Seeking; Callousness	Irresponsibility; Impulsivity; Distractibility; Rigid Perfectionism; Risk Taking	Unusual Beliefs and Experiences; Eccentricity; Perceptual Dysregulation;

Table 1. List of personality inventory for DSM-5 domains and facets.

Results
Demographic and psychiatric results

With respect to the PID-5 evaluation, comparisons between the BPD and HC samples revealed significantly increased impairment in patients with BPD across the greatest part of personality trait facets and all domain scores ($p < 0.01$). The mean domain scores obtained for the BPD and HC groups respectively were $1.91 (\pm 0.41)$ and $0.67 (\pm 0.52)$ for *Negative Affect*, $1.06 (\pm 0.5)$ and $0.47 (\pm 0.41)$ for *Detachment*, $0.90 (\pm 0.62)$ and $0.25 (\pm 0.32)$ for *Antagonism*, $1.56 (\pm 0.41)$ and $0.38 (\pm 0.31)$ for *Disinhibition* and $0.78 (\pm 0.39)$ and $0.19 (\pm 0.24)$ for *Psychoticism*, respectively. A table reporting all the group average scores for the PID-5 domains and facets and the significance of their difference between patients and controls is reported in Supplementary Table 1.

fMRI results

No subjects had to be removed from the data analysis due to excessive motion and there were no significant differences between patients (relative root mean square displacement = 0.05 ± 0.03 ; absolute = 0.23 ± 0.19) and controls (relative = 0.03 ± 0.01 ; absolute = 0.25 ± 0.16) in terms of motion during the acquisition.

The graph analysis of the FC matrices derived from the resting-state data demonstrated significant differences both at global and local levels.

At the global level, the dimension of the largest connected component, i.e., the number of nodes having at least one connection within the network, was significantly lower in patients than in HCs. There were no significant correlations between the global graph measures and the head motion during the fMRI acquisition, as shown in Supplementary Table 1.

At the nodal level, the centrality, measured by degree and strength, of several nodes in the limbic and frontotemporal regions was significantly altered between the two groups. The complete list of results is reported in Table 2 and is graphically represented in Fig. 1.

Correlation analyses

In the BPD group, significant correlations were found between the facet of *separation insecurity* and global efficiency ($R = 0.60$, adjusted- $p = 0.035$) and characteristic path length ($R = -0.60$, adjusted- $p = 0.035$). Additionally, a positive correlation emerged within the female BPD subgroup between the facet of *depressivity* and the degree of the left middle temporal gyrus ($R = 0.69$, adjusted- $p = 0.023$). Scatterplots of these correlations are shown in Supplementary Fig. 1.

Discussion

The aim of the present study was to assess whether the core psychopathological features of BPD are associated with different neurobiological alterations. By focusing on a sample of young adults at an early stage of the

Degree			Strength		
Region	Alteration	Adjusted p-value	Region	Alteration	Adjusted p-value
Right amygdala	BPD < HC	2.4×10^{-6}	Right thalamus	BPD > HC	1.4×10^{-3}
Left amygdala	BPD < HC	2.0×10^{-4}	Right caudate nucleus	BPD > HC	1.9×10^{-3}
Right caudate nucleus	BPD > HC	2.1×10^{-4}	Left thalamus	BPD > HC	6.8×10^{-3}
Right inferior temporal gyrus	BPD < HC	4.3×10^{-4}	Right caudal anterior cingulate	BPD > HC	9.2×10^{-3}
Left inferior temporal gyrus	BPD < HC	1.1×10^{-3}	Right paracentral gyrus	BPD > HC	1.3×10^{-2}
Right paracentral gyrus	BPD > HC	1.1×10^{-3}	Right pericalcarine cortex	BPD > HC	1.7×10^{-2}
Right thalamus	BPD > HC	1.1×10^{-3}	Left lingual gyrus	BPD > HC	3.2×10^{-2}
Right caudal anterior cingulate cortex	BPD > HC	3.5×10^{-3}	Left caudal anterior cingulate cortex	BPD > HC	3.7×10^{-2}
Left middle temporal gyrus	BPD < HC	3.8×10^{-3}	Left posterior cingulate cortex	BPD > HC	4.4×10^{-2}
Right pericalcarine cortex	BPD > HC	5.2×10^{-3}	Right lingual gyrus	BPD > HC	4.4×10^{-2}
Left thalamus	BPD > HC	9.3×10^{-3}	Left caudate nucleus	BPD > HC	4.8×10^{-2}
Left caudal anterior cingulate cortex	BPD > HC	1.1×10^{-2}	Right amygdala	BPD < HC	4.8×10^{-2}
Right hippocampus	BPD < HC	1.3×10^{-2}			
Right lingual gyrus	BPD > HC	1.4×10^{-2}			
Left pericalcarine cortex	BPD > HC	2.0×10^{-2}			
Left temporal pole	BPD < HC	2.1×10^{-2}			
Right middle temporal gyrus	BPD < HC	2.1×10^{-2}			
Right entorhinal cortex	BPD < HC	3.7×10^{-2}			
Right lingual gyrus	BPD > HC	4.5×10^{-2}			
Right lateral occipital cortex	BPD > HC	4.8×10^{-2}			
Left frontal pole	BPD < HC	4.8×10^{-2}			

Table 2. List of nodal features significantly altered between individuals with BPD and HCs. Differences between the two groups were observed in terms of centrality (degree and strength). The brain regions are reported in descending order of statistical significance.

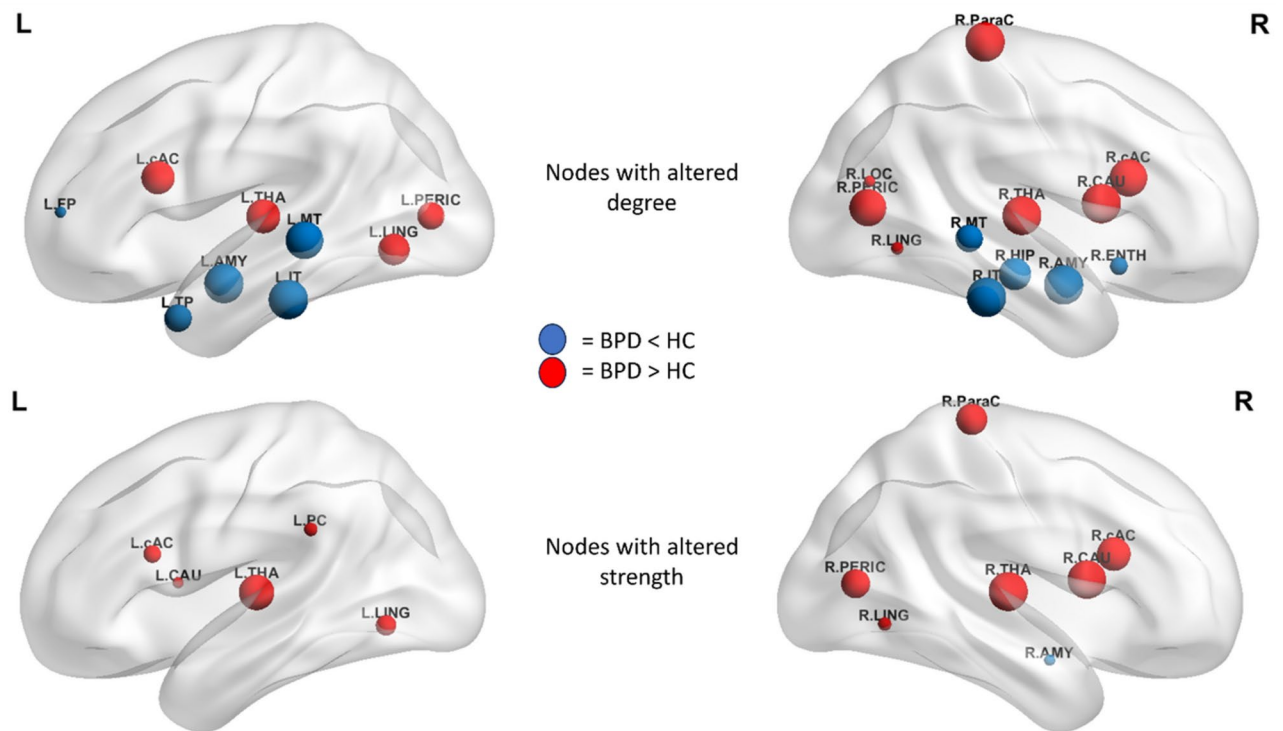


Fig. 1. Graphical representation of nodes with altered degree (top) and strength (bottom). The node size indicates greater statistical significance of the alteration. *L* left, *R* right, *AMY* amygdala, *CAU* caudate, *IT* inferior temporal, *ParaC* paracentral, *THA* thalamus, *cAC* caudal anterior cingulate, *MT* middle temporal, *PERIC* pericalcarine, *HIP* hippocampus, *LING* lingual, *TP* temporal pole, *ENTH* entorhinal, *LOC* lateral occipital, *FP* frontal pole, *PC* posterior cingulate.

disorder, we aimed to identify distinctive neurobiological patterns of BPD, unrelated to the comorbidities commonly arising in the advanced stages.

Despite the growing interest in functional brain imaging studies of personality disorders²⁴, research on the neurobiological networks implicated in BPD remains limited, and there is still little consensus on their possible correlations with specific psychopathological dimensions. Therefore, we adopted a graph analysis approach to investigate the whole-brain functional network at global and local levels.

Our exploratory findings, which are consistent with the alternative model for personality disorders proposed in the DSM-5-TR⁴, revealed a partial correlation between functional connectivity alterations and specific trait domains. Specifically, the facets of *separation insecurity* and *depressivity*, both within the *negative affectivity* domain⁴, showed significant correlations with alterations in brain connectivity. Notably, these correlations with global efficiency and characteristic path length measures and the degree of the left middle temporal gyrus remained significant after multiple comparisons.

Separation insecurity is defined as “fears of rejection by—and/or separation from—significant others, associated with fears of excessive dependency and complete loss of autonomy”. Since the introduction of BPD in the DSM-III, feelings of loneliness and emptiness, along with hypervigilance to rejection, have represented the core psychopathological features of this disorder²⁷. These features are mainly responsible for the inappropriate emotional dysregulation of BPD patients, particularly in response to perceived threats of separation or abandonment, which may not necessarily reflect actual events²⁸. Consistently, in the alternative DSM-5 model for personality disorders, *separation insecurity* was introduced as a diagnostic criterion for BPD⁴. This was further supported by a correlational observational study showing robust association between the dimensional item *separation insecurity* and the categorical BPD criterion *fear of abandonment*²⁹. Moreover, *separation insecurity* was identified as a distinguishing trait of BPD compared to other personality disorders in a cross-sectional study³⁰. Psychoanalytic theories suggest that the intolerance of loneliness and rejection in BPD arises from early developmental disruptions in the processes of separation and individuation³¹. Few authors have previously tried to find a neurobiological correlate for this important trait facet, and the issue remains open. For instance, in children, MRI data revealed that preschool separation anxiety was linked to reduced FC between the dmPFC and the vmPFC, with subsequent inhibition of the amygdala in response to fearful faces³². In BPD-specific research, a study investigating the neurobiological basis of *separation insecurity* and *fear of abandonment* using fMRI found that female BPD patients experiencing attachment distress presented increased ACC activation without effective top-down control of the dlPFC toward limbic structures³³. These findings suggest that hypoactivation of prefrontal areas, coupled with poor connectivity to limbic regions, may underlie the inability to regulate emotional responses. This dysregulation could explain why perceived rejection

easily triggers emotional disturbances in BPD. Additionally, an exploratory pilot study found that prefrontal dysfunction was associated with increased impulsivity and aggressiveness, further interfering with adherence and the effectiveness of pharmacological and psychotherapeutic interventions³⁴.

Taken together, these network impairments seem to underpin *separation insecurity*. This vulnerability may amplify fear of abandonment and rejection, which have been related to the intolerance of ambiguity observed in BPD in a cross-sectional research³⁵. Indeed, BPD patients share difficulties in recognizing and responding to neutral facial expressions, typically reacting with a negative affectivity³⁶. Based on this evidence, we can deduce that higher levels of *separation insecurity* correspond to a more pronounced dysfunction in interpreting social norms and managing interpersonal relationships. These difficulties likely contribute to impaired social functioning and diminished self-control, ultimately resulting in increased negative affective states such as anxiety and depressive symptoms.

Depressivity is intended as “frequent feelings of being down, miserable, and/or hopeless, difficulty recovering from such mood, pessimism about the future, pervasive shame, feelings of inferior self-worth, thoughts of suicide and suicidal behavior”. This dimension is particularly relevant in BPD, as evidenced by the high rate of comorbidity between BPD and major depressive disorder (MDD) documented in previous literature^{37–40}. Although both disorders share affective symptoms, it is still debated whether these symptoms differ in their underlying neurobiological networks. In the present study, we observed functional impairments in regions associated with the medial temporal network, including the middle and inferior temporal gyri and the amygdala. These findings are consistent with previous investigations examining the structural correlates of affective disturbances in BPD. For instance, prior research reported that patients with BPD showed greater GMV reductions in medial temporal regions, whereas patients with MDD tend to show more pronounced GMV reductions in frontostriatal regions^{41,42}. We propose that the predominant involvement of the medial temporal cortex in BPD may be explained by its anatomical and functional connections with the PFC, which are critical for the regulation of emotion and impulse control.

This distinctive neurobiological pattern may help clarify the subtle differences in depressive features observed in BPD compared to MDD. According to a review, depressivity in BPD is typically a reactive and impulsive experience of feeling miserable, lasting a few hours or days or, at most, a few weeks³⁸. Unlike MDD, where depressive episodes are more prolonged and persistent, BPD-related *depressivity* quickly changes according to the nature of the trigger event, resulting in BPD *depressivity*, an ontological instability that poorly responds to antidepressant medications³⁸. Further supporting our findings, another VBM study reported GMV reductions in different areas of the medial temporal cortex only in women with BPD and not in HCs, underscoring the unique neural signature of depressive symptoms in BPD⁴³.

From a clinical perspective, the observed correlations between separation insecurity, depressivity, and altered brain functional connectivity may highlight opportunities for early identification of BPD. Neurobiological signatures, particularly involving the middle temporal gyrus and global network efficiency, may be potential biomarkers for identifying vulnerable individuals in the early stages of the disorder. Early identification is particularly critical as BPD often develops during late adolescence or early adulthood, a window during which targeted interventions may yield the most significant and lasting benefits⁴⁴. By detecting neurobiological dysfunctions before full symptomatology manifests, clinicians may implement early, preventive strategies, potentially mitigating the course of the disorder. The correlation between the degree of the left middle temporal gyrus and *depressivity* identified exclusively in the female subgroup aligns with findings from prior research showing sex-specific differences in the neural correlates of BPD symptoms. For example, Soloff and colleagues⁴³ reported that women with BPD show GMV reductions in the temporal lobe compared to healthy females, a pattern not consistently observed in males. These differences may be partly explained by the neuroprotective effects of estrogen^{45,46}, which may modulate the function and connectivity of brain regions involved in emotional regulation. These brain alterations likely contribute to difficulties in interpreting social signals and regulating emotional responses, which are core features of the disorder, as supported by previous findings^{41,42}. Such findings emphasize the need for therapeutic interventions that address emotion recognition and interpersonal sensitivity.

Despite the novelty of this study, the results should be considered preliminary and interpreted in the context of some limitations. First, there are different methodological approaches for the investigation of brain functional connectivity, and from the same dataset, variable (and complementary) results may be obtained on the basis of the method used. Analogously, in the specific case of graph analysis, different definitions of nodes and edges of graphs may lead to different findings. Moreover, our sample size was limited and consisted predominantly of young females, precluding the examination of potential gender-based differences in network alterations. Therefore, gender-dependent conclusions drawn from our results (specifically) Future research should include larger and more diverse samples and consider additional analytical methods to strengthen the validity and generalizability of these findings.

To the best of our knowledge, this is the first study to correlate the PID-5 score in a BPD patient sample with functional neuroimaging results, expanding our knowledge on the “social brain”⁴⁷ and revealing potentially valuable insights towards the application of psychiatric therapy targeted at improving emotion regulation and social cognition. Our work revealed correlations between alterations in global network measures and in the middle temporal gyrus and the PID-5 facets of *separation insecurity* and *depressivity*. The delineation of specific neurobiological patterns is particularly interesting, as it provides promising avenues to further define the heterogeneity of BPD in different phenotypes with more homogenous psychopathological features and patterns of response to treatments.

Our results emphasize the need to correlate both structural and functional brain MRI patterns not only with the categorical diagnosis of BPD but also with dimensional features. From the earliest stages of the disease, specific psychopathological facets, which were explored in the present study through psychometric instruments such as the PID-5, may correlate with specific brain connectivity and functioning patterns. The latter may not

only provide a greater understanding of behavioral changes over time but also increase the possibility of tailoring psychotherapeutic and pharmacological treatment choices, predicting the response to these treatments from the perspective of increasing personalized and precision medicine. Similarly, patients could achieve higher levels of recovery, better integration, and quality of life. Therefore, we suggest that longitudinal studies aimed at assessing and correlating the evolution of clinical characteristics, as well as brain functional and structural neuroplasticity, would be of great interest.

We highlight the relevance of the graph analysis approach that generated hypotheses for future studies to strengthen the validity of the PID-5 to predict morphometric and functional neuroradiological patterns in BPD patients. We suggest extending this approach to further personality traits and domains of BPD and other personality disorders, thereby bridging the gap between psychopathology and neurobiology.

Methods

Participants

Twenty-eight patients with BPD (6M/22F, mean age = 23.7 ± 3.4 years, range = 18.9–30.3 years) and twenty-eight matched healthy controls (HCs) (6M/22F, mean age = 24.3 ± 2.8 years, range = 19.5–29.5 years) were included in this study. Our sample size, calculated using G*Power 3.1.9.7, showed a post-hoc power of 0.80 to detect differences of at least $d = 0.78$. Hence, smaller differences could not be detected⁴⁸. All patients were Italian speakers and received a formal psychiatric diagnosis of BPD through the Structured Clinical Interview for DSM-IV-Axis II (SCID-II)⁴⁹. These interviews were conducted by experienced professionals, including psychiatrists and clinical psychologists, to ensure diagnostic accuracy and reliability. To focus on core features of BPD and minimize the influence of other clinical factors, patients with current or past comorbid psychiatric diagnoses, including schizophrenia spectrum disorders, other personality disorders, and substance or alcohol use disorders, were excluded. Neurological disorders, intellectual disabilities, and continuous use of multiple psychotropic medications over the previous year were also exclusion criteria.

The study protocol was designed in accordance with the observance of the Code of Ethics of the World Medical Association (Declaration of Helsinki) and approved by the local Intercompany Ethics Committee of Bologna-Imola (Comitato Etico Interaziendale Bologna-Imola, CE-BI; #88866-24/07/2017). Written informed consent was obtained from all participants involved in the study.

The limbic system was previously studied in the same cohort via morphometry analysis (volumetry and cortical thickness) and seed-based analysis of resting-state fMRI data². Briefly, the study demonstrated a reduction in insula and amygdala volumes, as well as a decrease in the functional connectivity of the amygdala in individuals with BPD. These findings correlated with the clinical scales assessing emotion, rumination, and impulsivity regulation.

Psychiatric assessment

All participants underwent an extensive psychiatric assessment that included the following instruments:

- The Italian validation (Cronbach's $\alpha > 0.70$ for all PID-5 facet scales and > 0.90 for all PID-5 domain scales)³⁰ of the Personality Inventory for the DSM-5 (PID-5)⁵⁰ consists of 220 items for the assessment of maladaptive personality traits according to the alternative model for personality disorders. Each item can be assigned a Likert score from 0 = “always false/often false” to 3 = “always true/often true” (higher average scores indicate greater dysfunction in a specific personality trait facet or domain, whereas lower scores indicate an adaptive and resilient personality). These traits are described through 25 facets grouped into 5 high-order domains: negative affectivity, detachment, antagonism, disinhibition, and psychoticism. The total scores of the domains were calculated via the APA-all facets approach⁴.
- The Italian adaptation (Cronbach's $\alpha = 0.90$)⁵¹ of the Difficulties in Emotion Regulation Scale (DERS)⁵² is a 36-item self-report questionnaire that provides a comprehensive assessment of overall emotion dysregulation and evaluates the ability to modulate behavior according to individual goals and environmental requirements. It consists of six specific dimensions (i.e., nonacceptance of emotional responses, difficulties engaging in goal-directed behavior when distressed, impulse control difficulties when distressed, lack of emotional awareness, limited access to effective emotion regulation strategies, and lack of emotional clarity). Higher scores on the DERS indicate greater difficulty in emotion regulation.
- The Italian adaptation (Cronbach's $\alpha = 0.79$)⁵³ of the Barratt Impulsivity Scale (BIS-11)⁵⁴ is a 30-item self-report questionnaire that measures three dimensions of impulsivity: motor/behavioral impulsivity (i.e., the tendency to act “on the spur of the moment”, described by items such as “I buy things on impulses”), cognitive/attentional impulsivity (i.e., the failure to maintain concentration, expressed by items such as “I am restless at the theatre or lectures”) and nonplanning impulsivity (i.e., the tendency to act without thinking about the future consequences of action itself, through items such as “I am happy-go-lucky”). Self-reported scores are rated on a 4-point Likert scale, and the total scores range from 30 to 120, with higher scores indicating higher levels of impulsivity.
- The Self Harm Inventory (SHI)⁵⁵ is a 22-item, “yes/no” dichotomous, self-report instrument that explores participants' lifetime histories of self-harm behavior and severity of nonsuicidal self-injury, including eating disorders and high lethality. The SHI total score is obtained through the sum of affirmative responses and can be used both as a screening tool and to estimate the severity of self-harm. While no specific Italian validation was identified, the SHI was included for its broad applicability in clinical populations.
- The Italian adaptation (Cronbach's $\alpha = 0.90$)⁵⁶ of the Ruminative Response Scale (RRS)⁵⁷ is a 22-item self-report questionnaire designed to assess the tendency to engage in rumination when feeling sad, blue, or depressed. Self-reports are rated on a 4-point Likert scale, and the total score ranges from 22 to 88, with

higher scores indicating a greater degree of ruminative symptoms. Ruminative thinking is assessed along the dimensions of “brooding”, “reflection” and “depression”.

- The Italian adaptation (Cronbach's $\alpha = 0.85$)⁵⁸ of the Anger Rumination Scale (ARS)⁵⁹ is a 13-item self-report questionnaire designed to assess the tendency to focus attention on angry feelings, recall past anger experiences and contemplate their causes and consequences. Self-reports are rated on a 4-point Likert scale, with higher scores indicating a greater tendency to engage in anger rumination. The ARS is subdivided into four subscales: angry afterthought, thoughts of revenge, angry memories, and understanding of causes.
- The Italian validation (excellent internal consistency as measured by McDonald's Omega)⁶⁰ of the Edinburgh Handedness Inventory (EHI)⁶¹ quantifies hand dominance on a quantitative scale for ten habitual unimanual everyday acts. The participants are instructed to express their manual preference for each action by placing a “+” in the respective “left (L)” or “right (R)” column. They may also use “++” when they “would never try to use the other hand unless absolutely forced to”. In cases of ambidextrous preference, a “+” must be written in both columns. For scoring, 1 point is assigned to each “+”, and a laterality quotient (LQ) is calculated via the formula $LQ = (R - L) / (R + L) \times 100$. The LQ interval ranges from -100 (indicating total left-handedness) to $+100$ (indicating total right-handedness). Scores between -100 and -71 suggest left-handedness, scores between -70 and $+70$ indicate ambidexterity, and scores between $+71$ and $+100$ suggest right-handedness.
- The Beck Depression Inventory-II (BDI-II)⁶² was administered only to the BPD group. It is a 21-item self-administered questionnaire measuring the presence and severity of depressive symptoms during the past two weeks. A total score above 21 indicates a mild–moderate depressive state, whereas a score above 31 indicates a moderate–severe depressive state. The BDI-II was translated into Italian and the authors provided extensive data on the psychometric properties⁶³.

Note that, while all the mentioned scales were assessed for a complete characterization of the patient cohort, only the PID-5 was statistically evaluated in this work, as a novel scale whose neurobiological correlates have not been previously thoroughly investigated.

MRI data acquisition

Patients and HCs underwent a brain MR imaging protocol using a 1.5 T GE scanner (Signa HDx 15) with an 8-channel head coil. The MRI protocol included a 3D high-resolution T1-weighted image acquired via a fast spoiled gradient echo (FSPGR) sequence (pure axial orientation, TR/TE/T1 = 12.3/5.2/600 ms, FOV = 256 mm, 1 mm isotropic resolution) and a 9-min whole-brain resting-state fMRI scan acquired via a gradient EPI sequence (pure axial orientation, TR/TE = 3000/40 ms, FOV = 240 mm, 34 slices, $1.875 \times 1.875 \times 4$ mm³ resolution, 180 volumes). All the participants were instructed to stay in a relaxed state of wakefulness, keeping their eyes closed without falling asleep.

MRI data preprocessing

3D T1-weighted images were skull-stripped, and brain segmentation and parcellation were performed via FreeSurfer 5.3 (<https://surfer.nmr.mgh.harvard.edu/>) with the Desikan–Killiany atlas⁶⁴, resulting in 85 regions of interest (ROIs), including 8 bilateral subcortical ROIs, the bilateral cerebellum cortex and the brainstem.

The functional MRI data were preprocessed via a standardized pipeline developed in-house⁶⁵, which was based on FSL⁶⁶. Functional images were corrected for head motion using FSL mcflirt to align volumes to the central one; volumes with relative root mean square displacement higher than 1.5 mm were removed from the subject's sequence, and fMRI series with 25% or more volumes with excessive motion were excluded from the subsequent analysis; slice timing correction, spatial smoothing (Gaussian kernel FWHM = 6 mm) and a high-pass temporal filter (cutoff = 100 s) were applied; fMR volumes were linearly registered to 3D T1-weighted images, and the latter were nonlinearly warped to the Montreal Neurological Institute (MNI) template with a subsequent resampling to $2 \times 2 \times 2$ mm³. The functional images could then be aligned to MNI space by combining these two transformations. Independent component analysis was performed on the preprocessed data via FSL MELODIC. Noise components were manually classified by an expert following the guidelines provided by Griffanti and colleagues⁶⁷, and regressed out of the functional data.

Functional network construction and analysis

To generate the whole-brain functional connectome, graph nodes were defined for each subject as the 85 ROIs extracted from the FreeSurfer segmentation and parcellation of the brain. The ROIs were linearly registered to the functional images via trilinear interpolation, and the mean ROI time series was calculated as the weighted average of the voxel time series within that region. FC between nodes was defined as the Pearson correlation coefficient between the timeseries of each pair of nodes, thus generating one 85×85 FC graph per subject. The negative values were set equal to 0, as their interpretation is debated⁶⁸. The resulting graphs were proportionally thresholded, as a preferred method to absolute thresholding⁶⁹, at increasing connection density to preserve the 5–50% of the strongest connections within the network, with a step of 1%⁷⁰; the 5–50% density range was chosen as it was verified to be that where the property of small-worldness was satisfied¹⁹. The graphs were not binarized and were kept weighted for the subsequent analysis. The network construction procedure is summarized in Fig. 2.

Various network properties were evaluated to characterize the networks fully at both the global and nodal levels. Measures of segregation (modularity coefficient, clustering coefficient, local efficiency, and within-module z score), i.e., the ability for specialized processing to occur within densely interconnected groups of brain regions; integration (global efficiency, characteristic path length, and participation coefficient), i.e., the ability to rapidly combine specialized information from distributed brain regions; and centrality (degree, strength, and betweenness centrality), i.e., the importance of individual nodes within the network, were performed for each

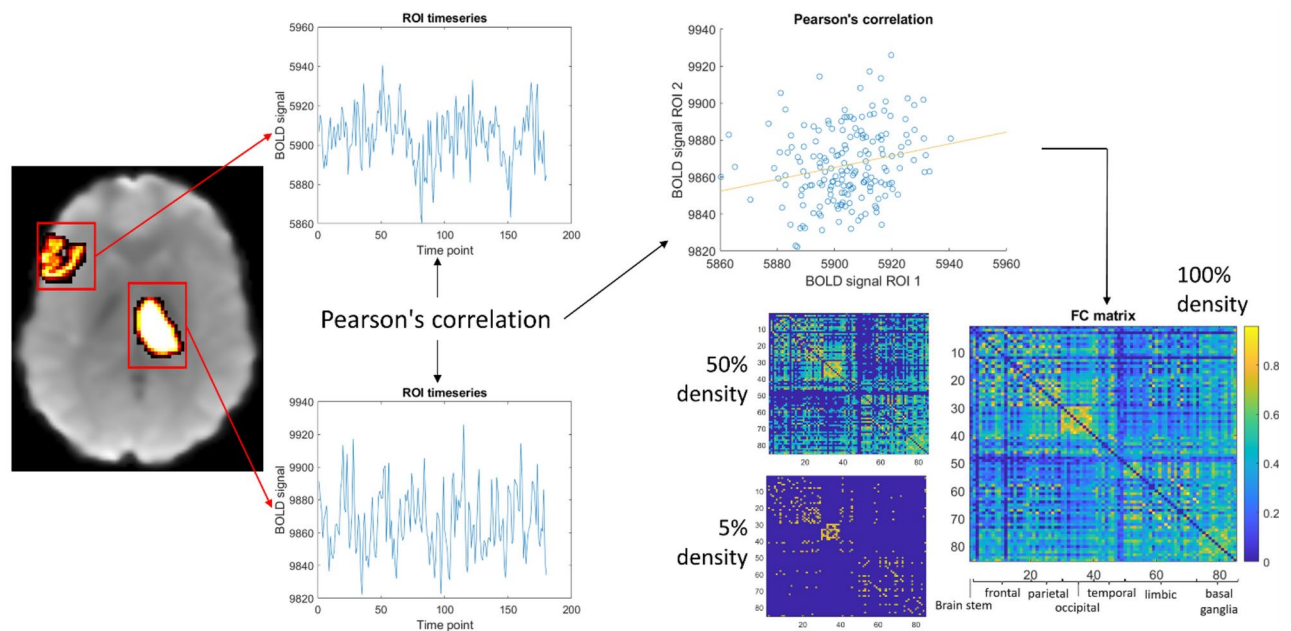


Fig. 2. Scheme of the functional connectivity network construction. The timeseries was extracted for each ROI, and Pearson's correlation between the ROI timeseries was subsequently calculated to define the connection (matrix element) between the ROIs. By calculating this quantity for each pair of ROIs, a functional connectivity (FC) matrix for each patient was obtained. Finally, the FC matrices were proportionally thresholded in the range of 5–50% of the network density.

patient at each threshold⁷¹. Each measure was then integrated within the density interval of 5–50% to obtain a single value per subject. Graph analysis was performed via the Brain Connectivity Toolbox (<https://sites.google.com/site/bctnet/>) in MATLAB R2019b. Network graphs were generated via the BrainNet viewer toolbox⁷².

Statistical analysis

The IBM “Statistical Package for the Social Sciences Software for Windows” (SPSS), version 22, was employed to perform the statistical analyses of the clinical data. Quantitative variables were compared through t-tests, which were separately performed on the average values of the main psychopathological ratings and of the PID-5 dimensions and facets. The statistical significance level was set at $p < 0.05$, and no statistical adjustment was performed.

A Shapiro–Wilk test was used to check the normality of the distribution of graph measures, and each property was compared between patients and HCs via ANCOVA with sex and age as covariates.

Pearson's correlation, partialling-out the effects of sex and age, was calculated between each global and local network measure and the average scores of the PID-5 5 domains and the 25 facets. This analysis was conducted in the full sample, in BPD patients only, and exclusively in female BPD patients, considering the skewed sex distribution.

The results were corrected for multiple comparisons via the false discovery rate approach. 35 PID-5 domains (sum and mean) and facets were corrected across each other; local graph metrics were corrected across the 10 graph metrics and the 85 network nodes; the 6 global measures were corrected across each other; Pearson's correlations between global network measures and PID-5 scores were corrected by 6 (global metrics) \times 30 (25 facets, 5 domain average); Pearson's correlations between local network measures and PID-5 scores were corrected by 10 (local metrics) \times 85 (nodes) \times 30. Statistical significance was set at adjusted- $p < 0.05$.

Ethical approval

The study was approved by the local Ethical Committee (#88866-24/07/2017), and written informed consent was obtained from all participants.

Data availability

The numerical data used to perform the statistical analysis in this work have been uploaded to the online repository Zenodo (<https://doi.org/10.5281/zenodo.13873759>) and can be accessed via prior and reasonable request to the Corresponding Author.

Received: 30 October 2024; Accepted: 6 January 2025

Published online: 12 April 2025

References

- Calvo, N. et al. Borderline personality disorder and personality inventory for DSM-5 (PID-5): Dimensional personality assessment with DSM-5. *Compr. Psychiatry* **70**, 105–111 (2016).
- Mitolo, M. et al. Emotion dysregulation, impulsivity and anger rumination in borderline personality disorder: the role of amygdala and insula. *Eur. Arch. Psychiatry Clin. Neurosci.* <https://doi.org/10.1007/s00406-023-01597-8> (2023).
- Leichsenring, F. et al. Borderline personality disorder: a comprehensive review of diagnosis and clinical presentation, etiology, treatment, and current controversies. *World Psychiatry* **23**, 4–25 (2024).
- American Psychiatric Association (APA). *Diagnostic and Statistical Manual of Mental Disorders* (APA Publishing, 2013).
- Keeley, J. W., Flanagan, E. H. & McCluskey, D. L. Functional impairment and the DSM-5 dimensional system for personality disorder. *J. Pers. Disord.* **28**, 657–674 (2014).
- Morey, L. C., McCredie, M. N., Bender, D. S. & Skodol, A. E. C. A. Level of personality functioning in the alternative DSM-5 model for personality disorders. *Pers. Disord. Theory Res. Treat.* **13**, 305–315 (2022).
- Fowler, J. C. et al. Clinical utility of the DSM-5 alternative model for borderline personality disorder: Differential diagnostic accuracy of the BFI, SCID-II-PQ, and PID-5. *Compr. Psychiatry* **80**, 97–103 (2018).
- Schulze, L., Schmahl, C. & Niedtfeld, I. Neural correlates of disturbed emotion processing in borderline personality disorder: a multimodal meta-analysis. *Biol. Psychiatry* **79**, 97–106 (2016).
- Davies, G., Hayward, M., Evans, S. & Mason, O. A systematic review of structural MRI investigations within borderline personality disorder: Identification of key psychological variables of interest going forward. *Psychiatry Res.* **286**, 112864 (2020).
- Grottaroli, M. et al. Microstructural white matter alterations in borderline personality disorder: A minireview. *J. Affect Disord.* **264**, 249–255 (2020).
- Shafie, M. et al. Resting-state functional magnetic resonance imaging alterations in borderline personality disorder: A systematic review. *J. Affect Disord.* **341**, 335–345 (2023).
- Dell'Osso, B., Berlin, H. A., Serati, M. & Altamura, A. C. Neuropsychobiological aspects, comorbidity patterns and dimensional models in borderline personality disorder. *Neuropsychobiology* **61**, 169–179 (2010).
- O'Neill, A. et al. Magnetic resonance imaging in patients with borderline personality disorder: a study of volumetric abnormalities. *Psychiatry Res.* **213**, 1–10 (2013).
- Nenadić, I., Voss, A., Besteher, B., Langbein, K. & Gaser, C. Brain structure and symptom dimensions in borderline personality disorder. *Eur. Psychiatr.* **63**, e9 (2020).
- Soloff, P. H. Structural brain abnormalities and suicidal behavior in borderline personality disorder. *J. Psychiatr. Res.* **46**, 516–525 (2012).
- Yang, X., Hu, L., Zeng, J., Tan, Y. & Cheng, B. Default mode network and frontolimbic gray matter abnormalities in patients with borderline personality disorder: A voxel-based meta-analysis. *Sci. Rep.* **6**, 34247 (2016).
- Sampedro, F. Structural brain abnormalities in borderline personality disorder correlate with clinical severity and predict psychotherapy response. *Brain Imaging Behav.* **15**, 2502–2512 (2021).
- Smitha, K. A. et al. Resting state fMRI: A review on methods in resting state connectivity analysis and resting state networks. *Neuroradiol. J.* **30**, 305–317 (2017).
- Bullmore, E. & Sporns, O. Complex brain networks: graph theoretical analysis of structural and functional systems. *Nat. Rev. Neurosci.* **10**, 186–198 (2009).
- Sporns, O. Graph theory methods: applications in brain networks. *Dialog. Clin. Neurosci.* **20**, 111–121 (2018).
- Xu, T. et al. Network analysis of functional brain connectivity in borderline personality disorder using resting-state fMRI. *Neuroimage Clin.* **11**, 302–315 (2016).
- Lei, X. et al. A resting-state fMRI study in borderline personality disorder combining amplitude of low frequency fluctuation, regional homogeneity and seed based functional connectivity. *J. Affect Disord.* **218**, 299–305 (2017).
- Lei, X. et al. Structural and functional connectivity of the anterior cingulate cortex in patients with borderline personality disorder. *Front. Neurosci.* **13**, 971 (2019).
- Sampedro, F. et al. A functional connectivity study to investigate the role of the right anterior insula in modulating emotional dysfunction in borderline personality disorder. *Psychosom. Med.* **84**, 64 (2022).
- Quattrini, G. et al. Abnormalities in functional connectivity in borderline personality disorder: Correlations with metacognition and emotion dysregulation. *Psychiatry Res. Neuroimaging* **283**, 118–124 (2019).
- Wolf, R. C. et al. Aberrant connectivity of resting-state networks in borderline personality disorder. *J. Psychiatry Neurosci.* **36**, 402–411 (2011).
- Reinhard, M. A., Nenov-Matt, T. & Padberg, F. Loneliness in personality disorders. *Curr. Psychiatry Rep.* **24**, 603–612 (2022).
- Matthies, S. et al. Please don't leave me-separation anxiety and related traits in borderline personality disorder. *Curr. Psychiatry Rep.* **20**, 83 (2018).
- Bach, B. & Sellbom, M. Continuity between DSM-5 categorical criteria and traits criteria for borderline personality disorder. *Can. J. Psychiatry* **61**, 489–494 (2016).
- Fossati, A. et al. Borderline personality disorder and narcissistic personality disorder diagnoses from the perspective of the DSM-5 personality traits: a study on Italian clinical participants. *J. Nerv. Ment. Dis.* **204**, 939–949 (2016).
- Coonerty, S. An exploration of separation-individuation themes in the borderline personality disorder. *J. Pers. Assess.* **50**, 501–511 (1986).
- Carpenter, K. L. H. et al. Preschool anxiety disorders predict different patterns of amygdala-prefrontal connectivity at school-age. *PLoS One* **10**, e0116854 (2015).
- Buchheim, A. et al. Neural response during the activation of the attachment system in patients with borderline personality disorder: an fMRI study. *Front. Hum. Neurosci.* **10**, 389 (2016).
- Soloff, P. H. et al. Impulsivity and prefrontal hypometabolism in borderline personality disorder. *Psychiatry Res.* **123**, 153–163 (2003).
- Nicholas Carleton, R., Sharpe, D. & Asmundson, G. J. G. Anxiety sensitivity and intolerance of uncertainty: Requisites of the fundamental fears?. *Behav. Res. Ther.* **45**, 2307–2316 (2007).
- Sato, M., Fonagy, P. & Luyten, P. Rejection sensitivity and borderline personality disorder features: A mediation model of effortful control and intolerance of ambiguity. *Psychiatry Res.* **269**, 50–55 (2018).
- Gunderson, J. G. et al. New episodes and new onsets of major depression in borderline and other personality disorders. *J. Affect Disord.* **111**, 40–45 (2008).
- Rao, S. & Broadbear, J. Borderline personality disorder and depressive disorder. *Australas Psychiatry* **27**, 573–577 (2019).
- Biskin, R. S., Frankenburg, F. R., Fitzmaurice, G. M. & Zanarini, M. C. Pain in patients with borderline personality disorder. *Personal Ment. Health* **8**, 218–227 (2014).
- Shah, R. & Zanarini, M. C. Comorbidity of borderline personality disorder: current status and future directions. *Psychiatr. Clin. N. Am.* **41**, 583–593 (2018).
- Cao, Y. et al. Common and distinct patterns of gray matter alterations in young adults with borderline personality disorder and major depressive disorder. *Eur. Arch. Psychiatry Clin. Neurosci.* **272**, 1569–1582 (2022).
- Depping, M. S. et al. Common and distinct structural network abnormalities in major depressive disorder and borderline personality disorder. *Prog. Neuropsychopharmacol. Biol. Psychiatry* **65**, 127–133 (2016).

43. Soloff, P., Nutsche, J., Goradia, D. & Diwadkar, V. Structural brain abnormalities in borderline personality disorder: A voxel-based morphometry study. *Psychiatry Res. Neuroimaging* **164**, 223–236 (2008).
44. Bozzatello, P., Bellino, S., Bosia, M. & Rocca, P. Early detection and outcome in borderline personality disorder. *Front. Psychiatry* **10**, (2019).
45. Pozzi, S., Benedusi, V., Maggi, A. & Vegeto, E. Estrogen action in neuroprotection and brain inflammation. *Ann. N. Y. Acad. Sci.* **1089**, 302–323 (2006).
46. Scala, M., Martínez Trapote, P., Rodríguez-Jiménez, R., Pecorino, B. & Serretti, A. Managing a treatment-resistant schizophrenia spectrum disorder with a hormonal twist in a female patient: a case report of a progestin-only pill. *J. Clin. Psychopharmacol.* **44**, 323–326 (2024).
47. Brothers, L. The social brain: a project for integrating primate behavior and neurophysiology in a new domain. <https://doi.org/10.7551/mitpress/3077.003.0029> (2002).
48. De Prisco, M. et al. Differences in facial emotion recognition between bipolar disorder and other clinical populations: A systematic review and meta-analysis. *Prog. Neuropsychopharmacol. Biol. Psychiatry* **127**, 110847 (2023).
49. First, M. B. & Gibbon, M. The structured clinical interview for DSM-IV Axis I disorders (SCID-I) and the structured clinical interview for DSM-IV Axis II disorders (SCID-II). In *Comprehensive Handbook of Psychological Assessment, Vol. 2: Personality Assessment* 134–143 (Wiley, 2004).
50. Krueger, R. F., Derringer, J., Markon, K. E., Watson, D. & Skodol, A. E. Initial construction of a maladaptive personality trait model and inventory for DSM-5. *Psychol. Med.* **42**, 1879–1890 (2012).
51. Sighinolfi, C., Norcini Pala, A., Chiri, L. R., Marchetti, I. & Sica, C. Difficulties in Emotion Regulation Scale (DERS): traduzione e adattamento italiano. (2010).
52. Gratz, K. L. & Roemer, L. 'Multidimensional assessment of emotion regulation and dysregulation: Development, factor structure, and initial validation of the difficulties in emotion regulation scale': Erratum. *J. Psychopathol. Behav. Assess.* **30**, 315–315 (2008).
53. Fossati, A., Di Ceglie, A., Acquarini, E. & Barratt, E. S. Psychometric properties of an Italian version of the Barratt Impulsiveness Scale-11 (BIS-11) in nonclinical subjects. *J. Clin. Psychol.* **57**, 815–828 (2001).
54. Patton, J. H., Stanford, M. S. & Barratt, E. S. Factor structure of the barratt impulsiveness scale. *J. Clin. Psychol.* **51**, 768–774 (1995).
55. Sansone, R. A., Wiederman, M. W. & Sansone, L. A. The self-harm inventory (SHI): Development of a scale for identifying self-destructive behaviors and borderline personality disorder. *J. Clin. Psychol.* **54**, 973–983 (1998).
56. Palmieri, R., Gapsar, A. & Lanciano, T. Una misura dispozionale della Ruminazione depressiva: la RRS di Nolen-Hoeksema e Morrow. *Psychofenia : Ricerca ed Analisi Psicologica* **0**, 15–33 (2007).
57. Nolen-Hoeksema, S. & Morrow, J. A prospective study of depression and posttraumatic stress symptoms after a natural disaster: The 1989 Loma Prieta earthquake. *J. Pers. Soc. Psychol.* **61**, 115–121 (1991).
58. Baldetti, M. & Bartolozzi, C. La Validazione Italiana dell'Anger Rumination Scale [Italian Validation of Anger Rumination Scale]. In *Studi Cognitivi, Cognitive Psychotherapy School and Research Centre* (2010).
59. Sukhodolsky, D. G., Golub, A. & Cromwell, E. N. Development and validation of the anger rumination scale. *Pers. Individ. Differ.* **31**, 689–700 (2001).
60. Gori, B., Grippo, A., Focardi, M. & Lolli, F. The Italian version of Edinburgh Handedness Inventory: Translation, transcultural adaptation, and validation in healthy subjects. *Laterality* **29**, 151–168 (2024).
61. Oldfield, R. C. The assessment and analysis of handedness: The Edinburgh inventory. *Neuropsychologia* **9**, 97–113 (1971).
62. Beck, A. T. An inventory for measuring depression. *Arch. Gen. Psychiatry* **4**, 561 (1961).
63. Sica, C. & Ghisi, M. The Italian versions of the Beck Anxiety Inventory and the Beck Depression Inventory-II: Psychometric properties and discriminant power. In *Leading-Edge Psychological Tests and Testing Research* 27–50 (Nova Science Publishers, 2007).
64. Desikan, R. S. et al. An automated labeling system for subdividing the human cerebral cortex on MRI scans into gyral based regions of interest. *NeuroImage* **31**, 968–980 (2006).
65. Evangelisti, S. et al. Brain functional connectivity in sleep-related hypermotor epilepsy. *Neuroimage Clin.* **17**, 873–881 (2018).
66. Jenkinson, M., Beckmann, C. F., Behrens, T. E. J., Woolrich, M. W. & Smith, S. M. FSL. *Neuroimage* **62**, 782–790 (2012).
67. Griffanti, L. et al. Hand classification of fMRI ICA noise components. *Neuroimage* **154**, 188–205 (2017).
68. Schwarz, A. J. & McGonigle, J. Negative edges and soft thresholding in complex network analysis of resting state functional connectivity data. *Neuroimage* **55**, 1132–1146 (2011).
69. van Wijk, B. C. M., Stam, C. J. & Daffertshofer, A. Comparing brain networks of different size and connectivity density using graph theory. *PLoS One* **5**, e13701 (2010).
70. Garrison, K. A., Scheinost, D., Finn, E. S., Shen, X. & Constable, R. T. The (in)stability of functional brain network measures across thresholds. *Neuroimage* **118**, 651–661 (2015).
71. Rubinov, M. & Sporns, O. Complex network measures of brain connectivity: Uses and interpretations. *NeuroImage* **52**, 1059–1069 (2010).
72. Xia, M., Wang, J. & He, Y. BrainNet viewer: a network visualization tool for human brain connectomics. *PLoS One* **8**, e68910 (2013).

Acknowledgements

The publication of this article was supported by the “Ricerca Corrente” funding from the Italian Ministry of Health.

Author contributions

E.D.A. and G.S. contributed equally to the data collection and/or analysis for this work, co-wrote the first draft and share first authorship. M.Mi., M.S., L.G., L.M., L.C., D.N.M. and C.T. contributed to the data acquisition and/or analysis and critically revised this manuscript. M.Me. and R.L. equally supervised this work and share last authorship. All the authors read and approved the final version of this manuscript.

Competing interests

The authors declare no competing interests.

Additional information

Supplementary Information The online version contains supplementary material available at <https://doi.org/10.1038/s41598-025-85989-x>.

Correspondence and requests for materials should be addressed to C.T.

Reprints and permissions information is available at www.nature.com/reprints.

Publisher's note Springer Nature remains neutral with regard to jurisdictional claims in published maps and institutional affiliations.

Open Access This article is licensed under a Creative Commons Attribution-NonCommercial-NoDerivatives 4.0 International License, which permits any non-commercial use, sharing, distribution and reproduction in any medium or format, as long as you give appropriate credit to the original author(s) and the source, provide a link to the Creative Commons licence, and indicate if you modified the licensed material. You do not have permission under this licence to share adapted material derived from this article or parts of it. The images or other third party material in this article are included in the article's Creative Commons licence, unless indicated otherwise in a credit line to the material. If material is not included in the article's Creative Commons licence and your intended use is not permitted by statutory regulation or exceeds the permitted use, you will need to obtain permission directly from the copyright holder. To view a copy of this licence, visit <http://creativecommons.org/licenses/by-nc-nd/4.0/>.

© The Author(s) 2025